X-621-71-214
PREPRINT

65565

IONOSPHERIC nf_H RESONANCES: FREQUENCY SHIFTS VS. PLASMA CONDITIONS

ROBERT F. BENSON

OCTOBER 1971

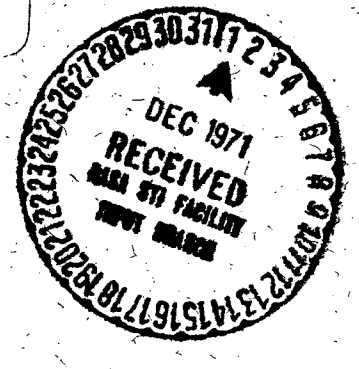

GSFC — GODDARD SPACE FLIGHT CENTER —
GREENBELT, MARYLAND

19

X-621-71-214

IONOSPHERIC nf_H RESONANCES: FREQUENCY SHIFTS VS. PLASMA CONDITIONS

Robert F. Benson

Thermosphere and Exosphere Branch
Laboratory for Planetary Atmospheres
NASA/Goddard Space Flight Center
Greenbelt, Maryland 20771

October 1971

ABSTRACT

The Alouette II resonances observed near the harmonics of the electron cyclotron frequency f_H reveal frequency shifts (relative to the nf_H values derived from model field calculations) which can be consistently interpreted in terms of plasma wave dispersion effects superimposed on a positive offset of several kilohertz in the Alouette II sounder transmitter frequency and a negative offset of a few ten's of gammas in the earth's magnetic field $|\vec{B}|$ (relative to the model field under quiet conditions near the magnetic equator). Plasma wave dispersion effects are observed on the $2f_H$ resonance when it is in the vicinity of the resonance observed near the upper hybrid frequency f_T. The $2f_H$ resonant frequency shift is positive when $f_T < 2f_H$ and negative when $f_T > 2f_H$. The observed shift is more than an order of magnitude greater than that expected from a matching of the group velocity of longitudinal plasma waves propagating perpendicular to $\vec{B}$, to the component of the satellite velocity perpendicular to $\vec{B}$. The observations suggest that an oblique echo model may be required to give a proper interpretation of the $2f_H$ resonance. Comparing the frequency shifts observed near f_T with theory indicates that cyclotron damping can be ignored only when the angle between the propagation vector $\vec{k}$ and the direction perpendicular to $\vec{B}$ is less than a few degrees for the $2f_H$ wave, and less than a few tenths of a degree for the nf_H waves with $n > 2$. The large positive frequency shifts previously attributed to the Alouette II f_H and $2f_H$ resonances can be explained by assuming a positive instrumental frequency offset. The negative offset of $|\vec{B}|$ inferred from the plasma resonance observations is consistent with expectations based on recent OGO 3 and OGO 5 rubidium magnetometer observations at higher altitudes in the equatorial regions.

1. INTRODUCTION

The Alouette I plasma resonances associated with the electron cyclotron frequency f_H and the harmonics nf_H ($n = 2, 3, 4, \cdots$) have been observed to deviate a few tenths of one percent from their expected frequency values based on model magnetic field calculations [Benson, 1970a]. The magnitude of the observed deviations varied with the harmonic number n; in addition, some of the frequency deviations appeared to depend upon the variations in the electron density N. An investigation of the data from Alouette II revealed that $f_n \rightarrow nf_H$ as n increases (where f_n is the frequency of the resonance associated with nf_H), and large positive shifts (of the order of 1%) were observed on the resonances near f_H and $2f_H$ [Benson, 1969]. These results were quite different from the Alouette I results where the deviation of f_n from nf_H increased with increasing n and where large positive shifts were not observed on the f_H and $2f_H$ resonances. In both of the above studies the expanded receiver amplitude vs. time format was used.

There are several differences in the Alouette I and Alouette II sounder systems which must be considered when comparing resonance data from the two satellites. The frequency response, frequency resolution, and the automatic gain control (AGC) are more suitable on Alouette II than on Alouette I for resonance investigation [Franklin, 1970; Franklin and Maclean, 1969; Benson, 1971b]. In addition, spring steel antenna elements were used on Alouette I while non-magnetic Be-Cu elements were used on Alouette II. Magnetic tests (which were conducted on a sample of the Alouette I antenna material) indicated that a contaminant field, capable of producing the observed Alouette I frequency deviations, was present out to a radial distance of a few meters from the antenna element (see pp. 44-45 of Benson [1970a]).

The difference between the observed frequency shifts on Alouette I and Alouette II for the higher nf_H resonances (typically $n \geq 6$) was attributed to the

above contaminant field, and it was concluded that the excitation region associated with these resonances extended only on the order of meters from the antenna [Benson, 1969]. No conclusions were obtained concerning the large positive frequency shifts observed on the Alouette II f_H and $2f_H$ resonances. Similar shifts of the Alouette II f_H resonance have been reported by Barry [1970] and can be recognized in the data presented in Figure 3 of Matuura, Nishizaki, and Nagayama [1969]; in these studies, large numbers of ionograms were analyzed in the conventional ionogram format.

The data for the present paper were chosen in order to investigate the above mentioned large positive Alouette II frequency shifts, and to investigate the N dependence of the frequency shifts seen on Alouette I. A proper interpretation of these frequency shifts is required before the resonances can be used with confidence in ionospheric measurements.

2. DISCUSSION OF NEW OBSERVATIONS

Frequency shift measurements of nf_H resonances. Four Alouette II satellite passes on magnetically quiet days (K_p = 0 or 1) were selected that corresponded to rapidly changing N along the orbital path while maintaining a nearly constant and low value of f_H for many consecutive ionograms. The projection of the subsatellite point on geographical coordinates is presented in Figure 1 during the time interval pertaining to the present data samples. The corresponding variations in the satellite height z are presented in Figure 2 together with the variations in $(\vec{V}_{sat})_\perp$, (the component of the satellite velocity perpendicular to the earth's magnetic field, $\vec{B}$), the electron temperature T_e (as obtained from the Alouette II probe experiment), and the plasma parameter f_N/f_H, where f_N is the electron plasma frequency. The quantity $(\vec{V}_{sat})_\perp$ is required to compare the frequency shift observations with

theoretical studies that include the motion of the satellite, T_e is required to calculate the group velocity $\vec{V}_g$ of the plasma waves that are considered to be the cause of the resonances, and f_N/f_H is of importance because it influences the shape of the dispersion curves associated with these plasma waves. The plasma parameter f_N/f_H is used as the abscissa in Figure 3, where the variation of f_H is presented, and in the presentation of the frequency shift measurements; f_N and f_H are related to N and B as follows:

$$[f_N\ (\text{kHz})]^2 \approx 81\ N\ (\text{cm}^{-3}) \tag{1}$$

and

$$f_H\ (\text{kHz}) \approx B\ (\gamma)/36. \tag{2}$$

The nearly constant f_H, over a wide range of f_N/f_H on each pass, corresponds to a series of ionograms with a pattern of nf_H resonances that remains nearly constant in frequency while the upper hybrid frequency f_T varies from $f_T < 2f_H$ to $f_T > 3f_H$, where $f_T^2 = f_N^2 + f_H^2$. This situation is ideal for the investigation of the dispersion of the nf_H plasma waves because the dispersion curves for these waves experience a dramatic change in shape as f_T crosses nf_H [e.g., see Crawford, 1965].

A precise frequency scaling of all nf_H resonances observed in the high frequency resolution portion of the ionograms (i.e., $nf_H < 2.0$ MHz) was performed on nearly all of the ionograms recorded on the above 4 passes over the region indicated in Figure 1. The conventional ionogram format was used to select the ionograms to be scaled, and the expanded receiver amplitude vs. time format was used in the actual scaling. The resonant center frequency could be scaled to an accuracy slightly better than 1 kHz when the frequency spectrum of the sounder pulse could be clearly recognized (see Figure 4); the method of scaling has been described previously [Benson, 1969]. The scaled frequency f_n was expressed in terms of a percent frequency shift defined as $(f_n - nf_H) \times 100/nf_H$

where f_H was determined from the Cain and Cain [1971] reference field. The observed shift was compared with the predicted shift based on the concept of matching $\vec{V}_g$ to the component of the satellite velocity parallel to $\vec{V}_g$. This matching concept was introduced by Shkarofsky and Johnston [1965] in an attempt to explain the long time durations observed for the Alouette I nf_H resonances. The comparison was made for cyclotron harmonic waves with the wave vector $\vec{k}$ satisfying the condition $\vec{k} \cdot \vec{B} = 0$, since these waves experience strong cyclotron damping when $\vec{k}$ deviates by more than a few degrees from this perpendicular orientation [Tataronis and Crawford, 1966]. The group velocity for these waves (which can be derived from Stix [Chap. 9, e.g. 105, 1962], e.g., see eq. 2 of Benson [1971b]) is also perpendicular to $\vec{B}$. The effect of allowing $\vec{k}$ to deviate slightly from the perpendicular orientation will be discussed in Section 4.

The results of the above comparison are presented in Figure 5 in the form of frequency shift in percent versus the plasma parameter f_N/f_H. The top 4 rows in Figure 5 present the results for each pass separately (f_H, $2f_H$, and $3f_H$ in the left, middle, and right columns respectively) and the bottom row presents a composite picture of all of the data. The dashed lines in the left column represent $(\vec{V}_{sat})_\perp$, the dashed lines in the middle and right columns (which almost merge with the zero line) represent the frequency shift corresponding to the matching conditions (see preceding paragraph) for $2f_H$ and $3f_H$, respectively. It is possible to obtain matching in the frequency region within a few percent of the cyclotron harmonics in either the low k or the high k portion of the plasma wave dispersion curve. The dashed lines for $2f_H$ and $3f_H$ correspond to the low k matching points (there is no low k matching point for perpendicular propagating plasma waves near f_H); the solid lines for f_H, $2f_H$, and $3f_H$ correspond to the high k matching points. The most outstanding features of Figure 5 are the following:

1. The average percentage frequency shift is positive for each nf_H resonance and it decreases with increasing n.

2. Large frequency deviations from the background level are observed on the $2f_H$ resonance when f_T is in the vicinity of $2f_H$; similar deviations are not observed on the $3f_H$ resonance when f_T is in the vicinity of $3f_H$. (Note: the arrows at the bottom of the figure designate the points where $f_T = 2f_H$ and where $f_T = 3f_H$.)

3. The observed frequency shifts do not agree with the expected shifts based on a matching of $\vec{V}_g$ to $(\vec{V}_{sat})_\perp$ for the low k (for $2f_H$ or $3f_H$) or the high k (for f_H, $2f_H$, or $3f_H$) matching points on the dispersion curves for cyclotron harmonic waves with $\vec{k} \cdot \vec{B} = 0$.

4. The positive frequency shifts cannot be interpreted strictly in terms of the Doppler shift $\vec{k} \cdot \vec{V}_{sat}$ (which becomes $k(\vec{V}_{sat})_\perp$ when $\vec{k} \cdot \vec{B} = 0$) since the variation of $(\vec{V}_{sat})_\perp$ is much greater than the observed shifts, e.g., on pass 4086 $(\vec{V}_{sat})_\perp$ varies by a factor of 7 while the observed frequency shift is nearly constant for each resonance (except for the $f_T \approx 2f_H$ portion of the $2f_H$ data). This statement is valid even if $\vec{k} \cdot \vec{B} \neq 0$ since cyclotron damping considerations, as discussed earlier, require that $\vec{k}$ remain within a few degrees of the perpendicular orientation.

The decreasing positive percentage frequency shift with increasing n suggests the possibility of a fixed instrumental frequency offset Δf since the percent error associated with f_H, $2f_H$, and $3f_H$ would then be $\Delta f/f_H$, $\Delta f/2f_H$, and $\Delta f/3f_H$ respectively. In order to investigate this possibility, the absolute frequency shifts in kilohertz for the f_H, $2f_H$, $3f_H$, and $4f_H$ resonances were plotted versus f_N/f_H for the two passes that contained high frequency resolution data for the $4f_H$ resonance. These absolute frequency shifts, which are presented in Figure 6, should be the same for each resonance if they are simply the result of an instrumental offset; the overall average values are seen to be about 4.9 kHz for f_H, 4.7 kHz for $2f_H$ (excluding the region from $f_N/f_H = 1.5$ to 2.0), 3.9 kHz for $3f_H$, and 1.4 kHz for

$4f_H$. The decreasing average value with increasing n may be the result of a difference between the model field and the true field, since such a difference has a greater effect on the higher harmonics, e.g., a 1 kHz difference in f_H represents a 4 kHz difference in $4f_H$; it will be shown in Section 3 that there is evidence for such a difference. If the zero line is moved up to approximately +5 kHz, then the direction of the $2f_H$ shift in the vicinity of f_T would be consistent with the change in the dispersion curve shape near this frequency (the dispersion curve is in the frequency range above $2f_H$ when $f_T < 2f_H$ and it is in the frequency range below $2f_H$ when $f_T > 2f_H$, e.g., see Crawford [1965]).

If the large average positive frequency shifts are the result of an instrumental effect rather than a plasma effect, then the shifts should be similar for different plasma conditions. This is seen to be the case in Figure 7 where the absolute shifts for the f_H, $2f_H$, and $3f_H$ resonances as observed on 2 perigee passes near the dip equator over South America, where f_N/f_H has its maximum value, are presented. (The overall average values are 5.4, 5.0, and 3.1 kHz for f_H, $2f_H$, and $3f_H$ respectively.) Similar comments hold for conditions corresponding to different latitudes as is illustrated by Figure 8 where the results for the f_H and $2f_H$ resonances, as observed in high northern latitudes, are presented. (The overall averages are 3.3 and 4.2 kHz for f_H and $2f_H$, respectively.)

Electron density gradient measurements. Similar conclusions concerning an instrumental offset are obtained by comparing the gradient of N parallel to $\vec{V}_{sat}$ as determined from consecutive ionograms with the gradient determined from a single ionogram. On pass 1927 several consecutive ionograms contained f_N resonances suitable for accurate frequency scaling [Benson, 1971a]; these resonances also contained well defined exit frequencies $f_x S$ of the x reflection trace. On this pass, the electron density gradient along the satellite path was found to be nearly constant (+.08% change in N per kilometer) over a distance of 480 km by comparing the calculated plasma frequency $(f_N)_{x,H}$ from three consecutive ionograms, where

$$[(f_N)_{x,H}]^2 = (f_xS)^2 - (f_xS)(f_H) \quad (3)$$

(f_xS was scaled from the ionograms and f_H was obtained from the Cain and Cain [1971] reference field; the conversion from plasma frequency to electron density is obtained from (1)). The above gradient, expressed as change in plasma frequency per second along the satellite path, was +0.89 ± 0.01 kHz/sec; thus the expected change in f_N during the 5.2 seconds that elapsed between the observation of the f_N resonance and the observation of f_xS on one ionogram was 4.6 kHz. The observed difference, however, was 11.0 ± 2.9 kHz. It is difficult to interpret this discrepancy in terms of ionospheric irregularities since similar results were obtained on each of the three ionograms. The discrepancy is removed by assuming a positive frequency offset Δf of the sounder system since the effect of Δf on the calculated plasma frequency $(f_N)_{x,H}$ in (3), via the scaled value f_xS, is not the same as it is on the value of f_N scaled directly from the f_N resonance as can be seen by rewriting (3) as

$$[(f_N)_{x,H}]^2 = [f_x S - \Delta f]^2 - [f_x S - \Delta f](f_H)$$

and comparing it with $(f_N - \Delta f)^2$ where f_N is the scaled f_N resonant frequency. The minimum value of Δf that will remove the discrepancy is about 7 kHz (for the ionogram recorded at 18:57:54 UT where the following scaled values were obtained: f_N = 314.4 ± .9 kHz, f_xS = 849.4 ± 1.1 kHz and the model field value for f_H was 724.7(5) ± .2 kHz). It is removed at a lower Δf value if the model field value for f_H is assumed to be too low; at the high latitude where this ionogram was recorded a value 1 kHz higher than the model value is not inconsistent with recent OGO-3 and 5 observations [M. Sugiura, personal communication, 1971]. The minimum value based on this slightly higher value of f_H is Δf = 4 kHz. Plasma wave dispersion effects should not significantly alter these results since the frequency shifts predicted for the f_N resonance are less than 1 kHz (McAfee, 1970) and the frequency shifts associated with f_xS are completely negligible since it is an electromagnetic wave rather than an electrostatic wave.

3. RE-EVALUATION OF EARLIER ALOUETTE II OBSERVATIONS

The above observations, both those based on the frequency shifts of the nf_H resonances and those based on the deduced gradient of N, are consistent with a frequency offset of the Alouette II sounder system by an amount $\Delta f \gtrsim 4$ kHz. These results require a re-evaluation of an earlier work [Benson, 1969] which did not consider the effect of an instrument offset. In this work the resonant frequency shift was expressed as a difference field $\Delta B = B_R - B_C$ where, from (2), $B_R(\gamma) \approx 36\, f_n\,(\text{kHz})/n$ is the magnetic field determined from f_n and the assumption $f_n = nf_H$, and B_c is the calculated reference field [Cain and Cain, 1971]; ΔB observations were made for resonances up to $8f_H$ (the maximum value for which high resolution observations can be made from Alouette II ionograms). The observed difference field ΔB can be expressed as

$$\Delta B = (\Delta B)_i + (\Delta B)_m + (\Delta B)_c + (\Delta B)_p \tag{4}$$

where

$(\Delta B)_i$ = ΔB resulting from an instrumental frequency offset

$(\Delta B)_m$ = ΔB due to inaccuracies in the model field

$(\Delta B)_c$ = ΔB due to magnetic contamination from the satellite and/or its antennas

$(\Delta B)_p$ = ΔB due to plasma wave dispersion effects.

The term $(\Delta B)_c$ is neglected on Alouette II since the magnetic contamination is restricted to the region within a few meters of the body of the satellite – a distance small compared to the antenna length. If the average positive frequency displacements of Figure 5 are assumed to be due to an instrumental offset, then the assumption $(\Delta B)_p \approx 0$ for all the nf_H resonances appears reasonable except for the $2f_H$ resonance when $f_T \approx 2f_H$; since $f_T \approx 3f_H$ for the data under consideration, the term $(\Delta B)_p$ will be neglected for $2f_H$ as well. In (4) let $(\Delta B)_i = 36\, \Delta f/n$, where Δf is the assumed instrumental offset, then

$$\Delta B(\gamma) \approx 36\, \Delta f\ (\text{kHz})\, \frac{1}{n} + \Delta B(\gamma)_m \tag{5}$$

The unknowns Δf and $(\Delta B)_m$ can be determined from two or more ΔB observations corresponding to different n values. The data points in Figure 9 were adapted from Figure 4 of Benson [1969], and the solid curves were obtained from a least squares fit of (5) to the ΔB values. Consider the data of Figures 9a and 9b first which correspond to individual ionograms from separate satellite passes. The above least squares fit corresponds to $\Delta f = 8.0$ kHz and $(\Delta B)_m = -50\gamma$ in (a) and to $\Delta f = 7.9$ kHz and $(\Delta B)_m = -51\gamma$ in (b). The averaged data corresponding to a series of consecutive ionograms from two separate passes are given in Figures 9c and 9d. The reference level curves, resulting from the above least squares fit, correspond to $\Delta f = 6.8$ kHz and $(\Delta B)_m - 40\gamma$ in (c) and to $\Delta f = 5.5$ kHz and $(\Delta B)_m = -16\gamma$ in (d).

The above negative $(\Delta B)_m$ values are consistent with the recent OGO 3 and OGO 5 rubidium magnetometer observations indicating a large inflation of the inner magnetosphere due to high energy plasma [Sugiura et al., 1970, 1971]. A more meaningful comparison with the above observations is obtained by removing the D_{st} corrections [Sugiura and Cain, 1969] which were applied to B_c in the present analysis (D_{st} represents the average magnetic storm field over all longitudes). The $(\Delta B)_m$ values corresponding to Figure 9 then become -41, -49, -41, and -5γ for (a), (b), (c), and (d) respectively. The larger negative offset associated with (a), (b), and (c) is consistent with the OGO observations that ΔB becomes more negative for weak disturbances than for quiet conditions (the K_p index was 2 for (a), (b), and (c) and 1 for (d)).

The above results indicate that the large positive frequency shifts reported earlier [Benson, 1969] for the n = 1 and n = 2 resonances (with $f_N/f_H \approx 3$) are consistent with a positive frequency offset Δf in the range of 5.5 to 8.0 kHz. The n = 2 resonance appears consistently below the reference level curves on all 4 passes by about 0.1 or 0.2% (a shift of about 9γ in Figure 9 is equivalent to a shift of 0.1%). This indication of a negative shift is consistent with the independent

observations of Figure 5 (based on 4 different Alouette II passes) near $f_N/f_H \approx 3$ where a slight depression with respect to the background level is apparent. [Note: The small positive shift associated with n = 4 in Figures 9a and 9c may be due to the presence of the f_{Q4} resonance [Warren and Hagg, 1968] which is sometimes observed slightly above $4f_H$ when $f_N/f_H \approx 3$ and was considered to be a possible cause for the relatively large scaling uncertainty associated with the $4f_H$ resonance [Benson, 1969]. Also, the indication of a small positive shift associated with n = 6 in Figure 9b may be due to scaling uncertainties introduced by the presence of a weak $2f_T$ resonance which was observed slightly above $6f_H$.]

4. INTERPRETATION OF OBSERVATIONS

Plasma wave dispersion effects. Plasma wave dispersion effects are observed on the $2f_H$ resonance when f_T is in the vicinity of $2f_H$. The frequency deviation of the $2f_H$ resonance from the background level is of the order of +1% when $f_T \lesssim 2f_H$ and of the order of -0.2% when $f_T \gtrsim 2f_H$ (see Figure 5). The larger frequency shift observed when $f_T < 2f_H$, as compared to $f_T > 2f_H$, is consistent with earlier Alouette I observations where the frequency of the $2f_H$ resonance was found to be very sensitive to variations in N when $f_T < 2f_H$ but not when $f_T > 2f_H$ [Benson, 1970a]. The expected frequency shifts based on the low k matching point of $\vec{V}_g$ to $(\vec{V}_{sat})_\perp$ is less than .01% in absolute value when f_T is near $2f_H$ (the expected shift is positive when $f_T < 2f_H$ and negative when $f_T > 2f_H$). The longitudinal plasma wave group velocity (for waves propagating perpendicular to $\vec{B}$) corresponding to the largest positive frequency shift values of Figure 5 is of the order of 150 km/sec (which is about 30 times larger than $(\vec{V}_{sat})_\perp$ for the above observations). The corresponding group velocity in the region of $f_N/f_H \approx 1.6$, where the frequency shift is approximately 0.5%, is of the order of 80 to 90 km/sec; in the region of $f_N/f_H \approx 1.9$, where the frequency shift is approximately -0.2%, it is of the order of -50 to -60 km/sec. These large values (relative to $(\vec{V}_{sat})_\perp$) suggest that the $2f_H$ resonance may be the result of longitudinal plasma waves with

the above starting velocities that give rise to oblique echoes in a manner similar to the generation of the f_N resonance [McAfee, 1968, 1969a; Aubry, Bitoun, and Graff, 1970; Fejer and Yu, 1970; McAfee, 1970; Bitoun, Graff, and Aubry, 1970; Warnock, McAfee, and Thompson, 1970; Graff, 1971; Benson, 1971a] and the f_T resonance [McAfee, 1969b; Aubry, Bitoun, and Graff, 1970; Bitoun, Graff, and Aubry, 1970; Graff, 1970].

Similar plasma wave dispersion effects are not observed on the $3f_H$ resonance, i.e., the resonant frequency changes by less than 0.2% as f_T changes from $f_T < 3f_H$ to $f_T > 3f_H$ (see Figure 5). This is in conflict with earlier conclusions based on Alouette I observations [Benson, 1970a]. The present Alouette II observations are considered more reliable for the following reasons: (1) the frequency resolution is greater on Alouette II than on Alouette I, (2) there are more than 5 times as many observations in the Alouette II data sample corresponding to the condition $f_T > 3f_H$ than there are in the Alouette I data sample, and (3) the Alouette II data is free from the effect of magnetic contamination due to the antenna elements.

Instrumental offset. The non-zero reference level for the nf_H resonances in Figure 5 can be consistently interpreted in terms of an instrumental offset Δf between +4 and +8 kHz. The reference point for this offset figure is the leading edge of the frequency marker (as determined from the expanded amplitude time format) with the -3.0 ± 0.3 kHz frequency marker correction term included, e.g., the leading edge of the 1.5 MHz marker is considered to be at 1.497 ± .0003 MHz (for a discussion of frequency scaling accuracy see Benson [1970b]). Since the present frequency measurements are based on the observed resonant frequency structure, which is caused by the frequency spectrum of the transmitted pulse, the frequency offset is attributed to a positive shift of the Alouette II transmitter frequency relative to the frequency markers. This offset is not of great importance to standard ionospheric measurements, e.g., the maximum error in the determination of N in the vicinity of the satellite would be approximately +8% corresponding to $\Delta f = 8$ kHz

and $f_N \approx 0.2$ MHz; it can cause large errors, however, in the determination of B from the resonance observed near f_H (almost 300γ). It should be noted that the corrections required to compensate for a linear interpolation between the frequency markers [Benson, 1970b] are in the same direction as those required to compensate for the offset.

The lack of large positive frequency shifts on the Alouette I resonances at f_H and $2f_H$ (see Figure 4a of Benson [1970a]) suggests that either a similar instrumental offset was not present on Alouette I or that the offset was compensated for by the action of the AGC. The latter possibility seems more likely since the Alouette I and Alouette II frequency control systems are similar [C. Franklin, private communication 1971], and the short AGC time constant on Alouette I (12 msec on attack and 46 msec on decay) would have a larger effect on the strong resonances corresponding to low n values than on the weaker resonances at high n values. The action of the AGC would cause a strong resonance (such as f_H, $2f_H$, or $3f_H$) to be scaled too low in frequency since the reaction to the early pulses of the resonance (a typical resonance is composed of 10 or more sounder pulses) would reduce the receiver gain for the later pulses; the net effect would be to skew the resonant profile toward a lower frequency.

Cyclotron damping considerations. If the positive frequency shifts observed in the present data – and in the data of Benson [1969], Barry [1970], and Figure 3 of Matuura, Nishizaki, and Nagayama [1969] – are interpreted in terms of an instrumental offset, then the deviation of the resonant frequency from the ambient value in the medium is less than a few tenths of 1% except for the $2f_H$ resonance when $2f_H \approx f_T$. In particular, the frequency deviations on the higher harmonic resonances are less than 0.1%, i.e., less than 9γ on Figure 9. Thus deviations from perpendicular propagation are strongly affected by cyclotron damping which can be neglected only when

$$\left| \frac{(f_n - n f_H)}{k_{||}} \left(\frac{m_e}{2 \kappa T_e} \right)^{1/2} \right| >> 1 \qquad (6)$$

where $k_{||}$ is the component of $\vec{k}$ parallel to $\vec{B}$, m_e is the electron mass and κ is Boltzmann's constant [e.g., see Tataronis and Crawford, 1966]. An estimate of the propagation angle corresponding to (6) can be obtained for the $2f_H$ resonance where frequency shifts attributed to plasma wave dispersion effects were observed. Rewriting (6) as

$$k_{||} R << \left| \left(\frac{f_n - n f_H}{n f_H} \right) \frac{n}{2^{3/2} \pi} \right|,$$

where $R = (\kappa T_e / m_e)^{1/2} / (2\pi f_H)$ is the electron cyclotron radius, and setting $|f_n - nf_H| / nf_H = 0.002$ and $n = 2$ (corresponding to $f_N / f_H = 1.84$ on pass 1927 of Figure 5) gives $k_{||} R << 4.5 \times 10^{-4}$. An estimate of the corresponding value for $k_\perp R$ can be obtained from the dispersion equation for perpendicular propagation (e.g., see eq. 105 of Chap. 9 of Stix [1962]); the result is $k_\perp R \approx 2.5 \times 10^{-2}$ which corresponds to an angular deviation of only 1° from perpendicular propagation. Thus the propagation direction for the $2f_H$ wave must be well within 1° of the direction perpendicular to $\vec{B}$ in order to ignore cyclotron damping effects when $f_T \gtrsim 2f_H$. When $f_T \lesssim 2f_H$, where frequency deviations as large as 1% are observed, the corresponding angle is approximately 3°. For higher harmonics of f_H the angle becomes considerably smaller, e.g., it is approximately .2° for $3f_H$ when $f_T \approx 3f_H$ and $(f_n - nf_H)/nf_H = .002$ (the actual angle may be even smaller because frequency shifts as large as .2%, which is approximately the observational limit on the data of Figure 5, were not observed). Thus the largest deviation from the condition $\vec{k} \cdot \vec{B} = 0$, that is consistent with negligible cyclotron damping, occurs on the $2f_H$ wave. When $\vec{k} \cdot \vec{B} \neq 0$, it is no longer true that $\vec{V}_g$ is parallel to $\vec{k}$ and it is necessary to match $\vec{V}_g$ to $\vec{V}_{sat}$ rather than to $(\vec{V}_{sat})_\perp$. The predicted frequency shift, however, is still less than .01% which is to be compared with an observed shift of approximately 1%. As previously mentioned,

the discrepancy suggests that an oblique echo mechanism may be responsible for the observed resonance at $2f_H$.

ACKNOWLEDGMENTS

I gratefully acknowledge the assistance of the Information Processing Division of GSFC in the analog to digital data conversion process. I am grateful to Mr. J. E. Jackson for many helpful discussions and critical comments. I am also grateful to Mr. L. H. Brace for providing electron temperature values as obtained from the Alouette II probe experiment, to Dr. H. Oya for many stimulating discussions, to Dr. S. J. Bauer for helpful comments throughout the course of the work, and to Dr. M. Sugiura for his assistance in comparing the plasma resonance observations with the OGO observations.

I am grateful to Dr. C. A. Franklin and Mr. J. Matsushita of the Communications Research Centre, Ottawa, for helpful discussions pertaining to the Alouette I and Alouette II frequency control system.

REFERENCES

Aubry, M. P., J. Bitoun, and P. Graff, Propagation and group velocity in a warm magnetoplasma, Radio Sci., 5, 635-645, 1970.

Barry, J. D., Frequency shift in ionogram gyrofrequency resonance, Proc. IEEE, 58, 1869-1870, 1970.

Benson, R. F., Frequency shifts observed in the Alouette II cyclotron harmonic plasma resonances, Proc. IEEE, 57, 1139-1142, 1969.

Benson, R. F., An analysis of Alouette I plasma resonance observations, in Plasma Waves in Space and in the Laboratory, NATO Advanced Study Institute, Røros, Norway, April 17-26, 1968, Proceedings Vol. 2, Edited by J. O. Thomas and B. J. Landmark, pp. 25-54, Edinburgh University Press, Edinburgh, 1970a.

Benson, R. F., Frequency interpolation correction for Alouette II ionograms, Proc. IEEE, 58, 1959-1960, 1970b.

Benson, R. F., Alouette 2 observations supporting the oblique echo model for the plasma frequency resonance, J. Geophys. Res., 76, 1083-1087, 1971a.

Benson, R. F., Ionospheric plasma resonances: time durations vs. latitude, altitude, and f_N/f_H, presented at the URSI-IUPAP Symposium on Waves and Resonances in Plasmas, St. John's Newfoundland, 5-9 July 1971, NASA/ Goddard Space Flight Center, Greenbelt, Md.. X-621-71-253, Oct. 1971b.

Bitoun, J., P. Graff, and M. Aubry, Ray tracing in warm magnetoplasma and applications to topside resonances, Radio Sci., 5, 1341-1349, 1970.

Cain, J. C., and S. Cain, Derivation of the international geomagnetic reference field [IGRF (10/68)], NASA Technical Note D-6237, 1971.

Crawford, F. W., A review of cyclotron harmonic phenomena in plasma, Nuclear Fusion 5, 73-84, 1965.

Fejer, J. A., and Wai-Mao Yu, Excitation of plasma resonances by a small pulsed dipole in a weakly inhomogeneous plasma, J. Geophys. Res., 75, 1919-1925, 1970.

Franklin, C. A., and M. A. Maclean, The design of swept-frequency topside sounders, Proc. IEEE, 57, 897-929, 1969.

Franklin, C. A., Alouette experimental equipment for detecting resonances and VLF signals, in Plasma Waves in Space and in the Laboratory, NATO Advanced Study Institute, Røros, Norway, April 17-26, 1968, Proceedings, Vol. 2, Edited by J. O. Thomas and B. J. Landmark, pp. 3-23, Edinburgh University Press, Edinburgh, 1970.

Graff, Ph., Analytical study of oblique echoes at the upper hybrid resonance, J. Geophys. Res., 75, 7193-7198, 1970.

Graff, Ph., General expression of the frequencies of the oblique echoes at the plasma resonance, J. Geophys. Res., 76, 1060-1064, 1971.

Matuura, N., R. Nishizaki, and M. Nagayama, Analysis of observational data obtained by Alouette II, III. Proton cyclotron echoes in the topside ionograms, J. Radio Res. Laboratories, 16, 207-213, 1969.

McAfee, J. R., Ray trajectories in an anisotropic plasma near plasma resonances, J. Geophys. Res., 73, 5577-5583, 1968.

McAfee, J. R., Topside resonances as oblique echoes, J. Geophys. Res., 74, 802-808, 1969a.

McAfee, J. R., Topside ray trajectories near the upper hybrid resonance, J. Geophys. Res., 74, 6403-6408, 1969b.

McAfee, J. R., Topside plasma frequency resonance below the cyclotron frequency, J. Geophys. Res., 75, 4287-4290, 1970.

Shkarofsky, I. P., and T. W. Johnston, Cyclotron harmonic resonances observed by satellites, Phys. Rev. Letters, 15, 51-53, 1965.

Stix, T. H., The theory of plasma waves, McGraw-Hill, Inc., New York, 1962.

Sugiura, M. and S. J. Cain, Provisional hourly values of equatorial D_{st} for 1964, 1965, 1966, and 1967, NASA Goddard Space Flight Center, Greenbelt, Maryland X-621-69-20, February, 1969.

Sugiura, M., T. L. Skillman, B. G. Ledley, and J. P. Heppner, Magnetic field observations in high β regions of the magnetosphere, in Particles and Fields in the Magnetosphere, Edited by B. M. McCormac, pp. 165-170, Springer-Verlag New York Inc., New York, 1970.

Sugiura, M., B. G. Ledley, T. L. Skillman, and J. P. Heppner, Magnetospheric field distortions observed by OGO's 3 and 5, NASA/Goddard Space Flight Center, Greenbelt, Maryland, X-645-71-203, May 1971.

Tataronis, J. A., and F. W. Crawford, Cyclotron and collision damping of propagating waves in a magneto-plasma, Proceedings of the 7th International Conference on Phenomena in Ionized Gases, Belgrad, August 1965, II, pp. 244-247 Ed. by B. Perović and D. Tošić, Gradevinska Knjiga Pub. House, Belgrad, 1966.

Warnock, J. M., J. R. McAfee, and T. L. Thompson, Electron temperature from topside plasma resonance observations, J. Geophys. Res., 75, 7272-7275, 1970.

Warren, E. S., and E. L. Hagg, Observations of electrostatic resonances of the ionospheric plasma, Nature, 220, 466-468, 1968.

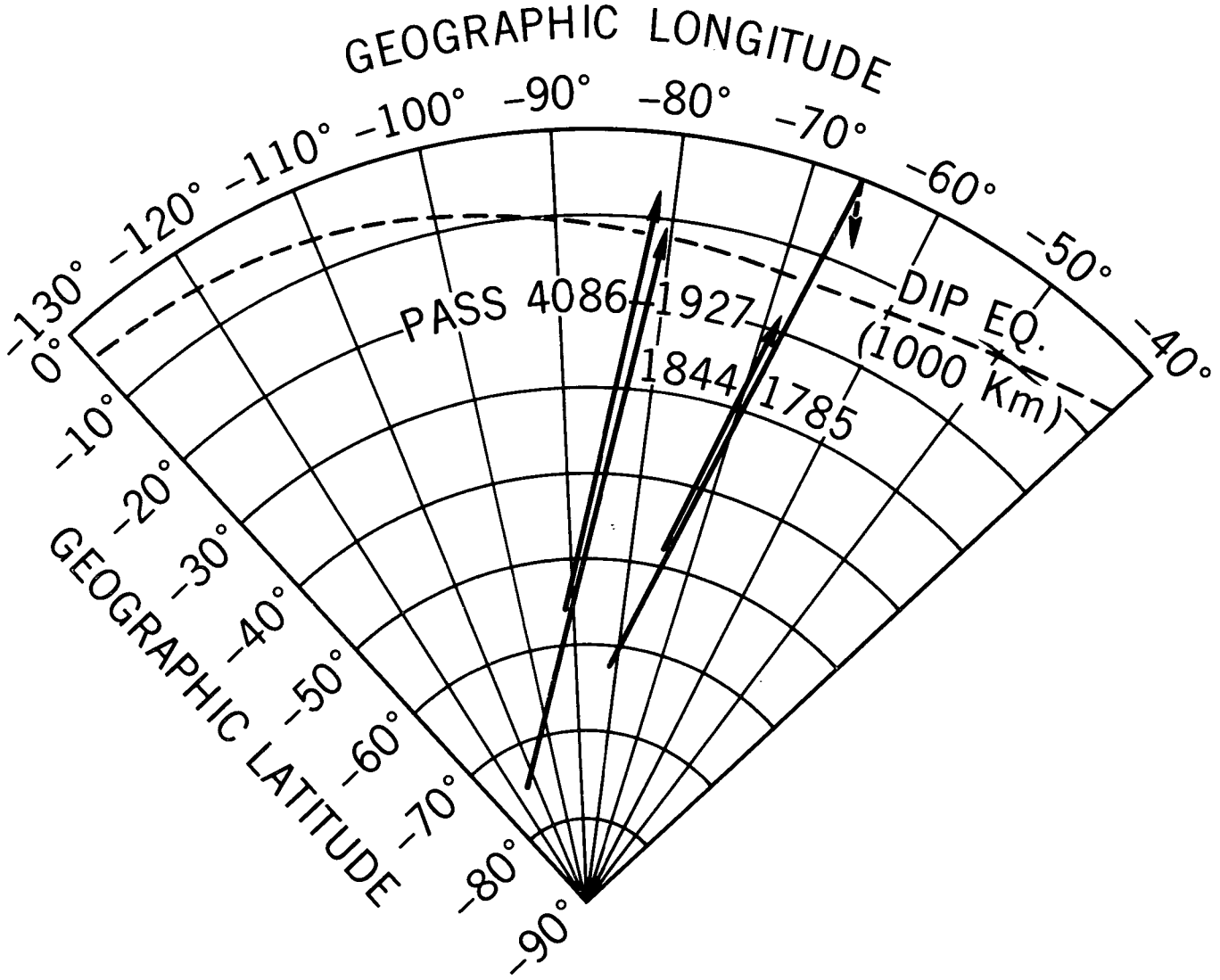

Figure 1. Geographic location of the portions of 4 Alouette II passes used in the present study. The lengths of the arrows correspond to the time intervals given in Figure 2.

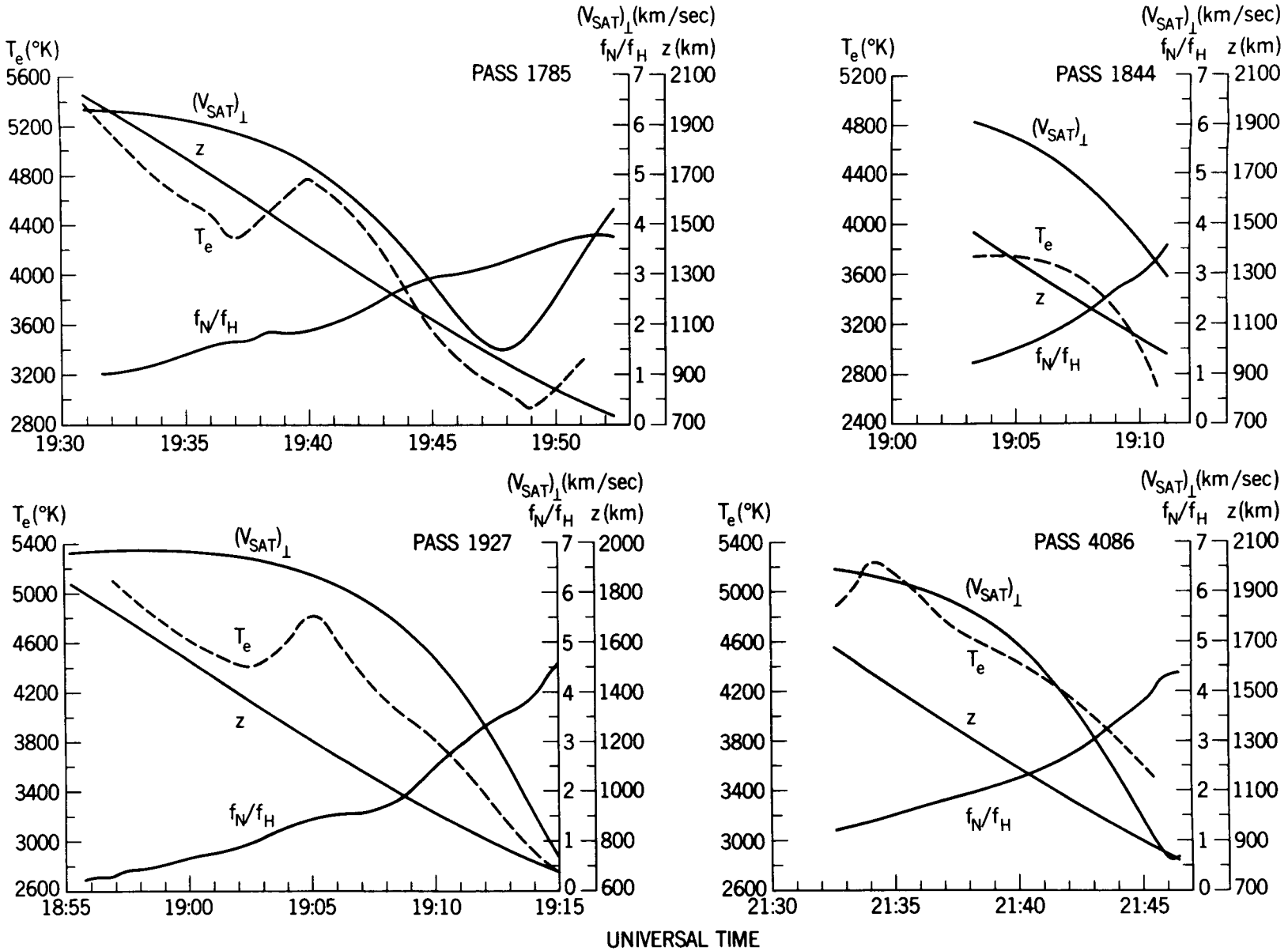

Figure 2. Variations of orbital and plasma parameters as a function of UT corresponding to the satellite path segments of Figure 1. The first right hand scale is used for $(\vec{V}_{sat})_\perp$ and (f_N/f_H); the second right hand scale is used for the height z. The pass numbers correspond to the following dates in 1966: 28 April, 3 May, 10 May, and 8 November for passes 1785, 1844, 1927, and 4086, respectively.

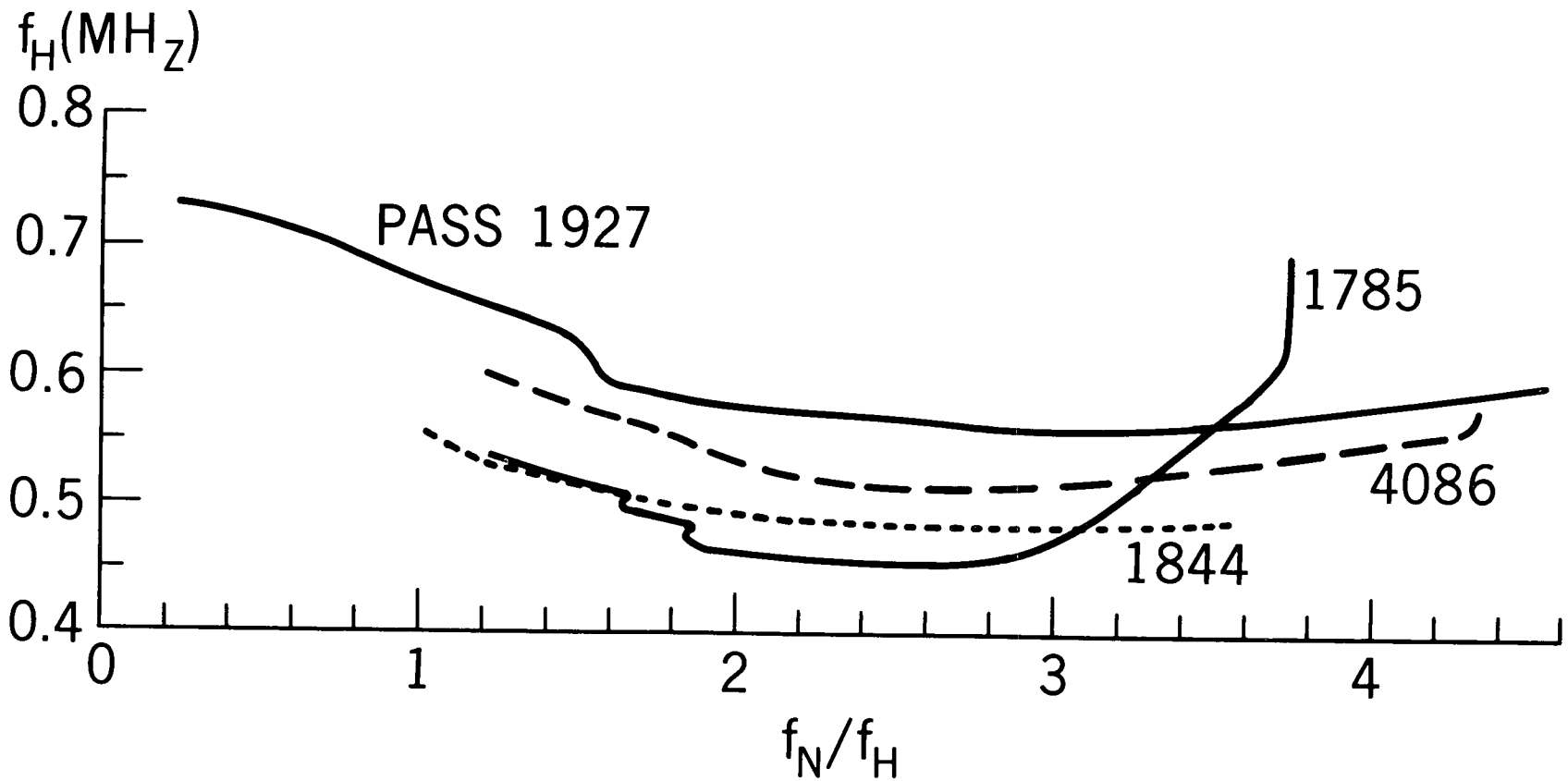

Figure 3. Variation of f_H as a function of the plasma parameter f_N/f_H corresponding to the values given in Figure 2.

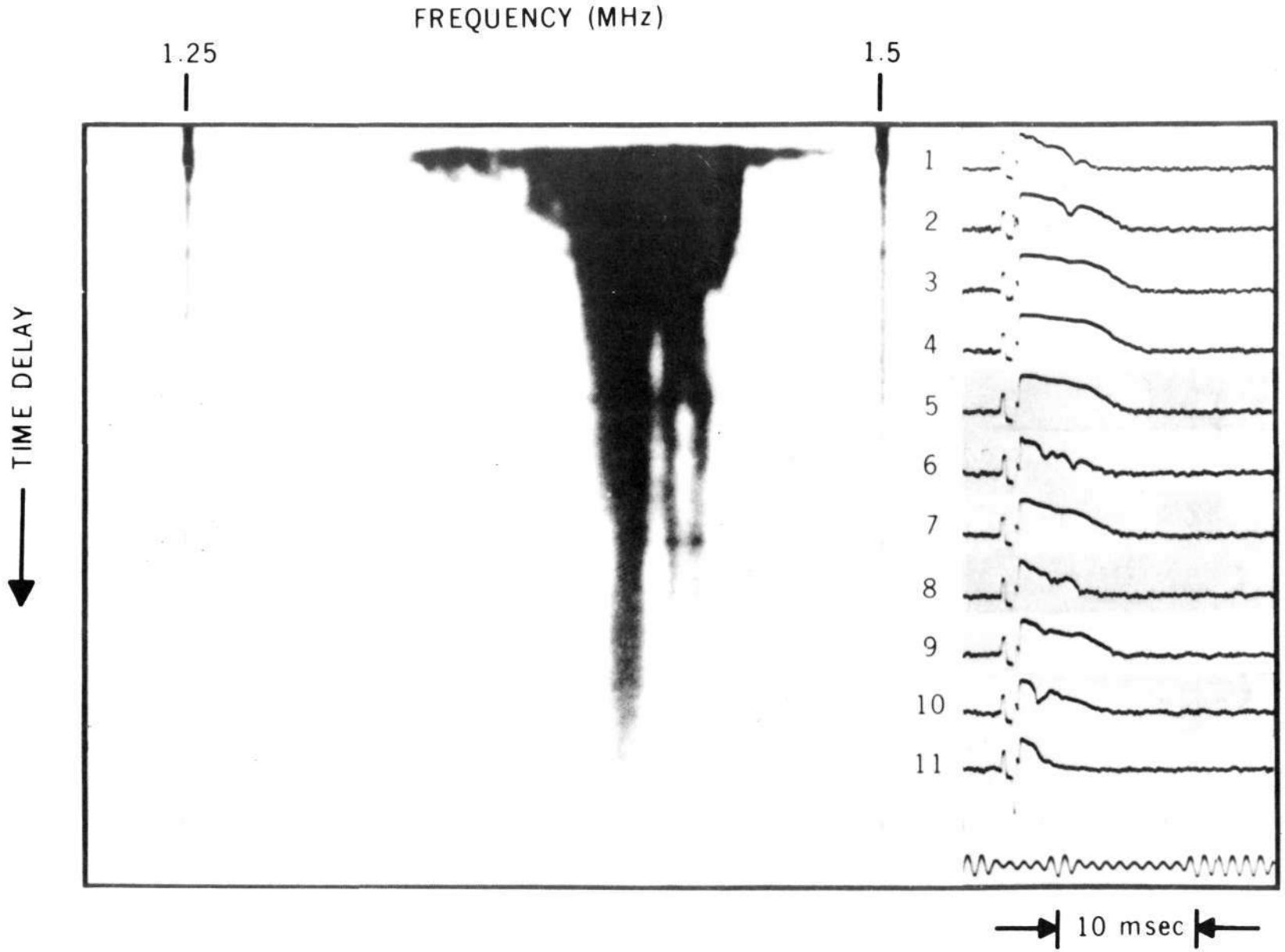

Figure 4. The $2f_H$ resonance in the ionogram format (left) and a portion of the resonance (11 consecutive sounder pulses) in the receiver amplitude vs. time format (right). The two deep minima observed on the ionogram format are caused by the frequency spectrum of the 100 μsec sounder pulse. These relatively small signal returns correspond to the receiver output following pulses 6 and 8 on the receiver amplitude vs. time format. The signal below pulse 11 is a 1 kHz time code signal. The resonance was taken from an Alouette II ionogram recorded at Quito at 19:52:23 UT on 28 April 1966 (pass 1785).

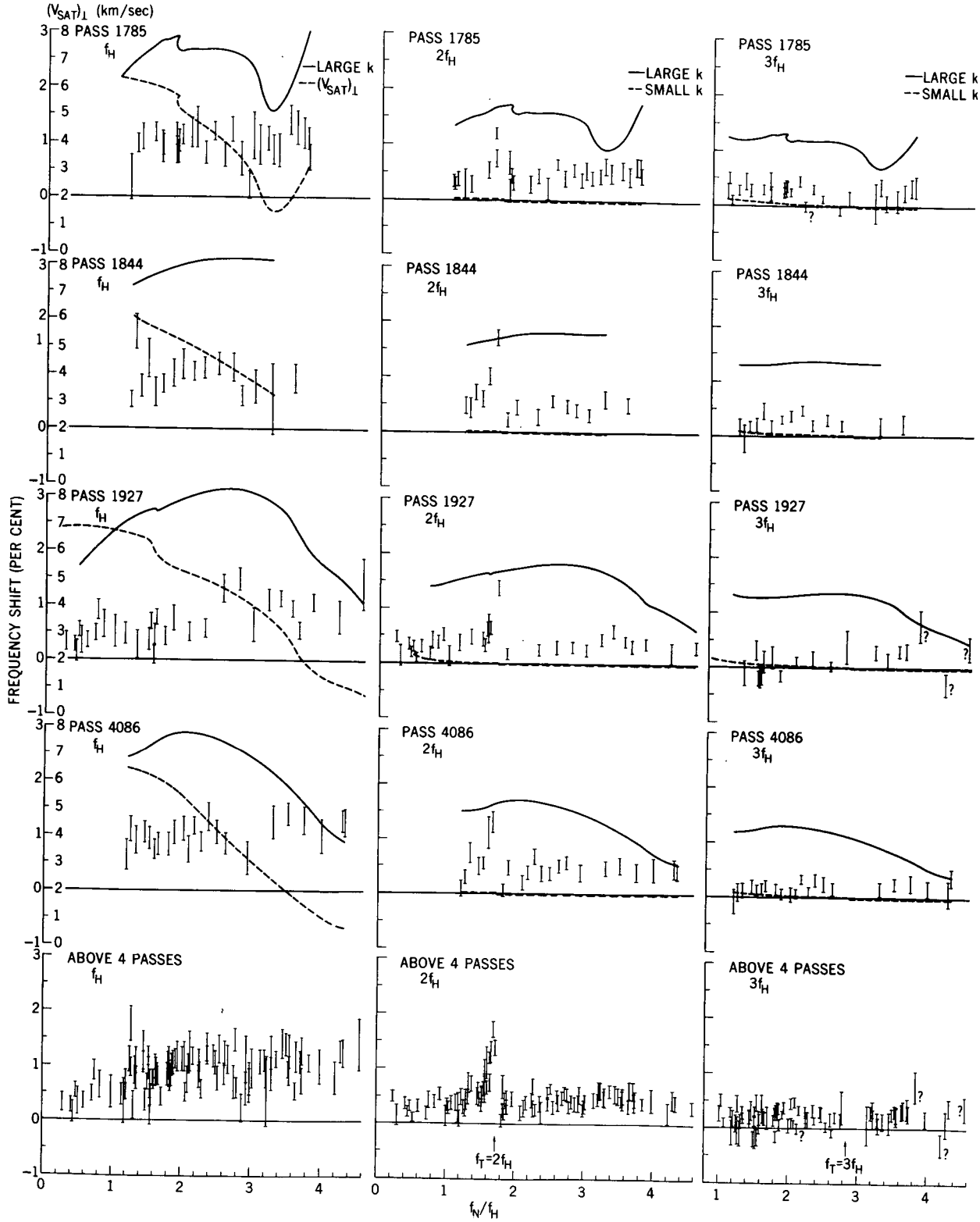

Figure 5. Observed frequency shift in percent vs. f_N/f_H for the f_H, $2f_H$, and $3f_H$, resonances observed on the 4 Alouette II passes of Figure 1. The shifts expected from a matching of $\vec{V}_g$ to $(\vec{V}_{sat})_\perp$ in the small and large k portions of the dispersion curves for $\vec{k} \cdot \vec{B} = 0$ together with $\vec{V}_{sat})_{\perp,}$ are also presented. The dashed curves in the $2f_H$ and $3f_H$ columns, corresponding to $\vec{V}_g = (\vec{V}_{sat})_\perp$ in the small k region, change from positive to negative when $f_T = nf_H$; the scale for these curves has been exaggerated slightly in order to show this change.

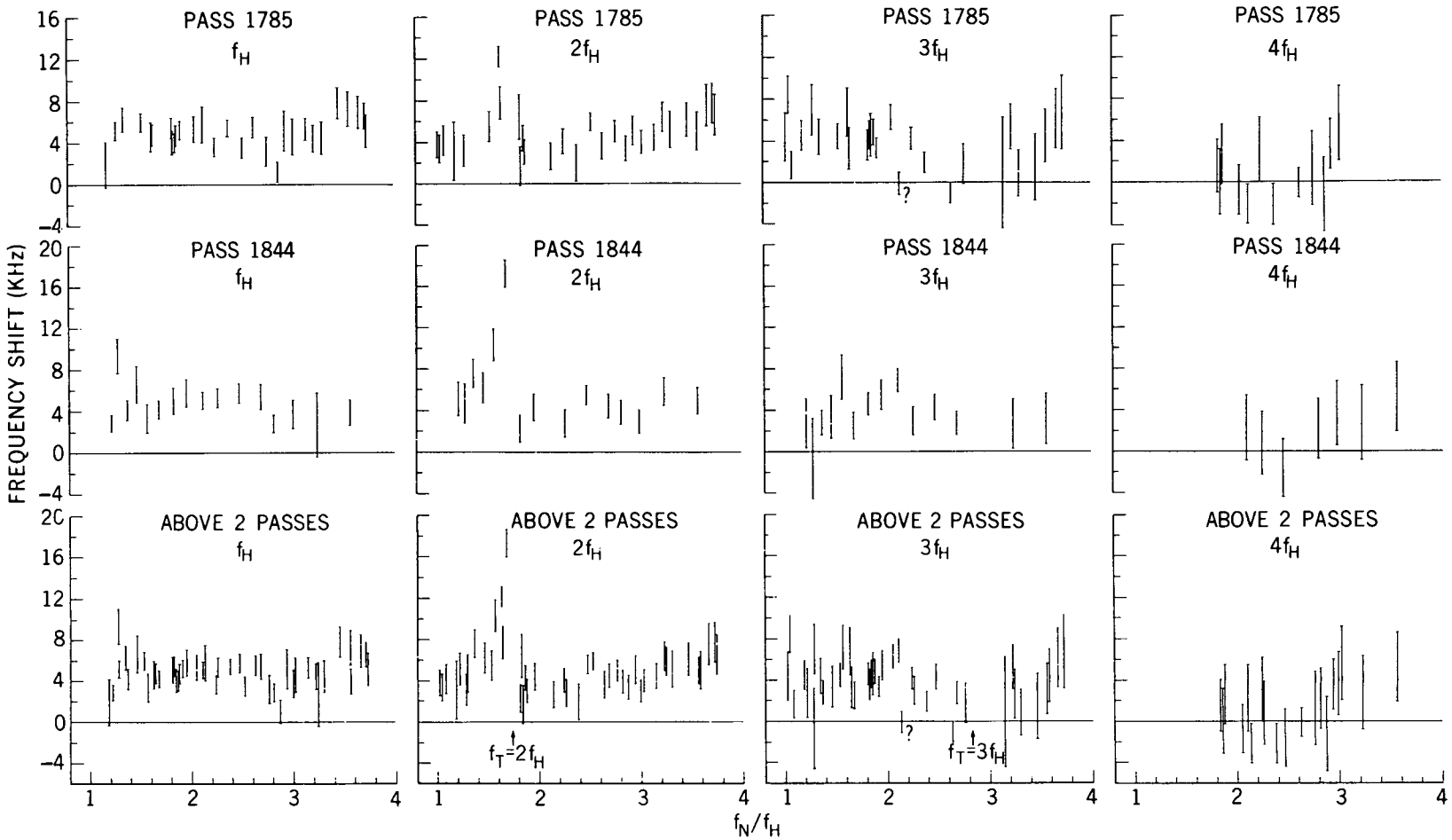

Figure 6. Observed frequency shift in kilohertz vs. f_N/f_H for the f_H, $2f_H$, $3f_H$, and $4f_H$ resonances from two of the passes of Figure 5.

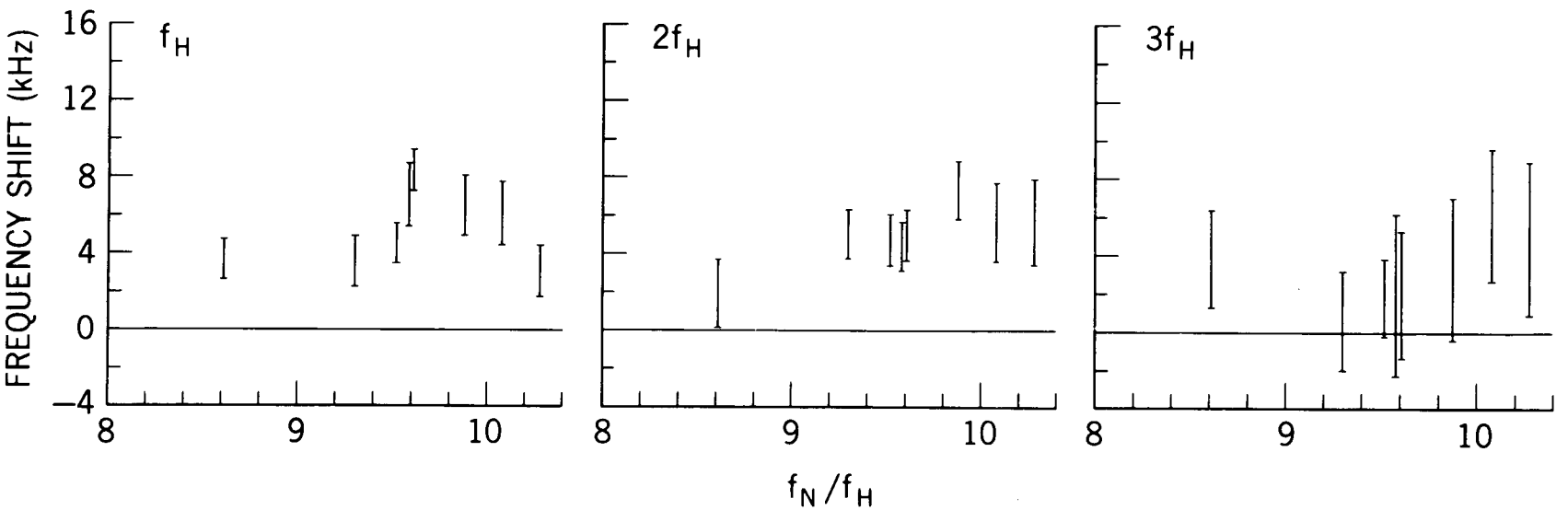

Figure 7. Observed frequency shift in kilohertz vs. f_N/f_H for the f_H, $2f_H$, and $3f_H$ resonances from two perigee passes near the dipole equator (3 ionograms from Quito pass 2151 [16:39:52 to 16:40:57 UT on 29 May 1966] and 5 ionograms from Quito pass 2210 [16:03:41 to 16:05:51 on 3 June 1966]).

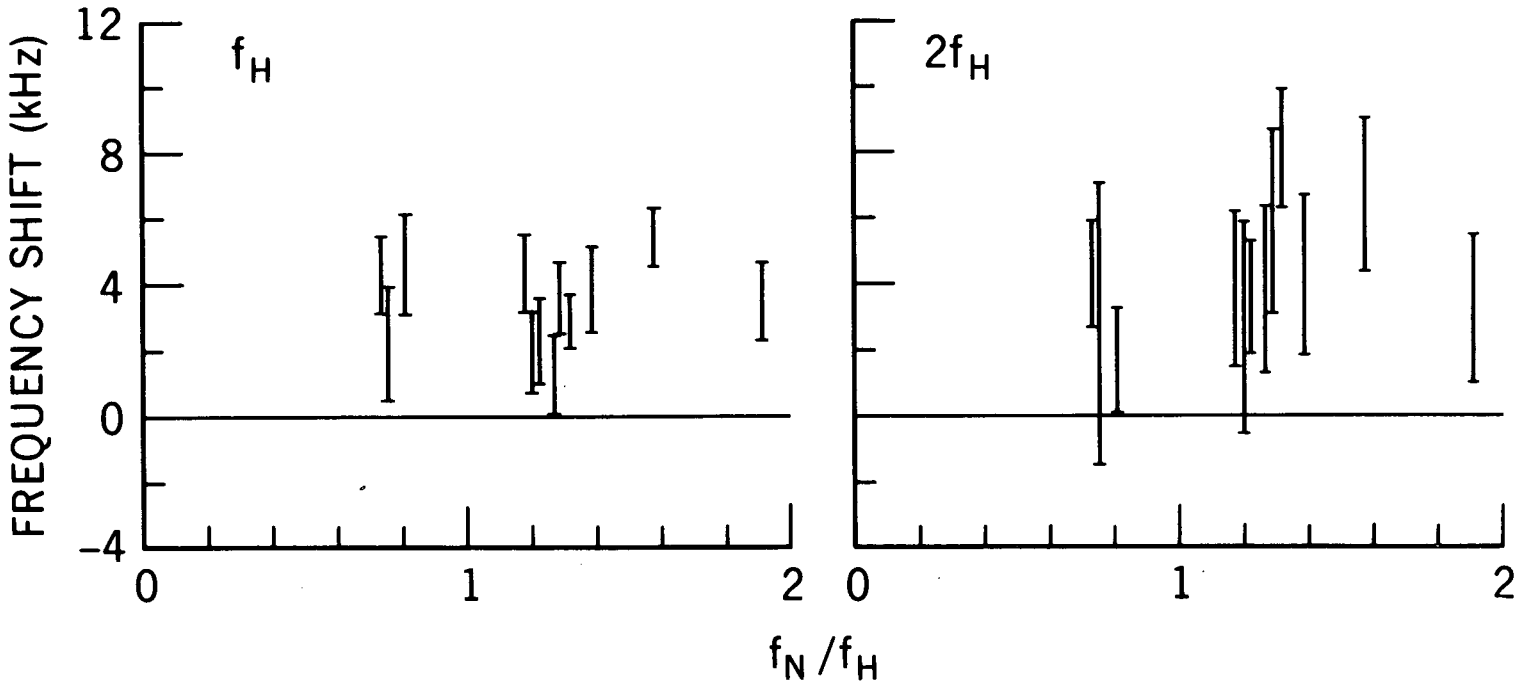

Figure 8. Observed frequency shift in kilohertz vs. f_N/f_H for the f_H and $2f_H$ resonances from four Ottawa passes (12 ionograms from passes 6719, 6743, 6754, and 6755 [18-21 June 1967]).

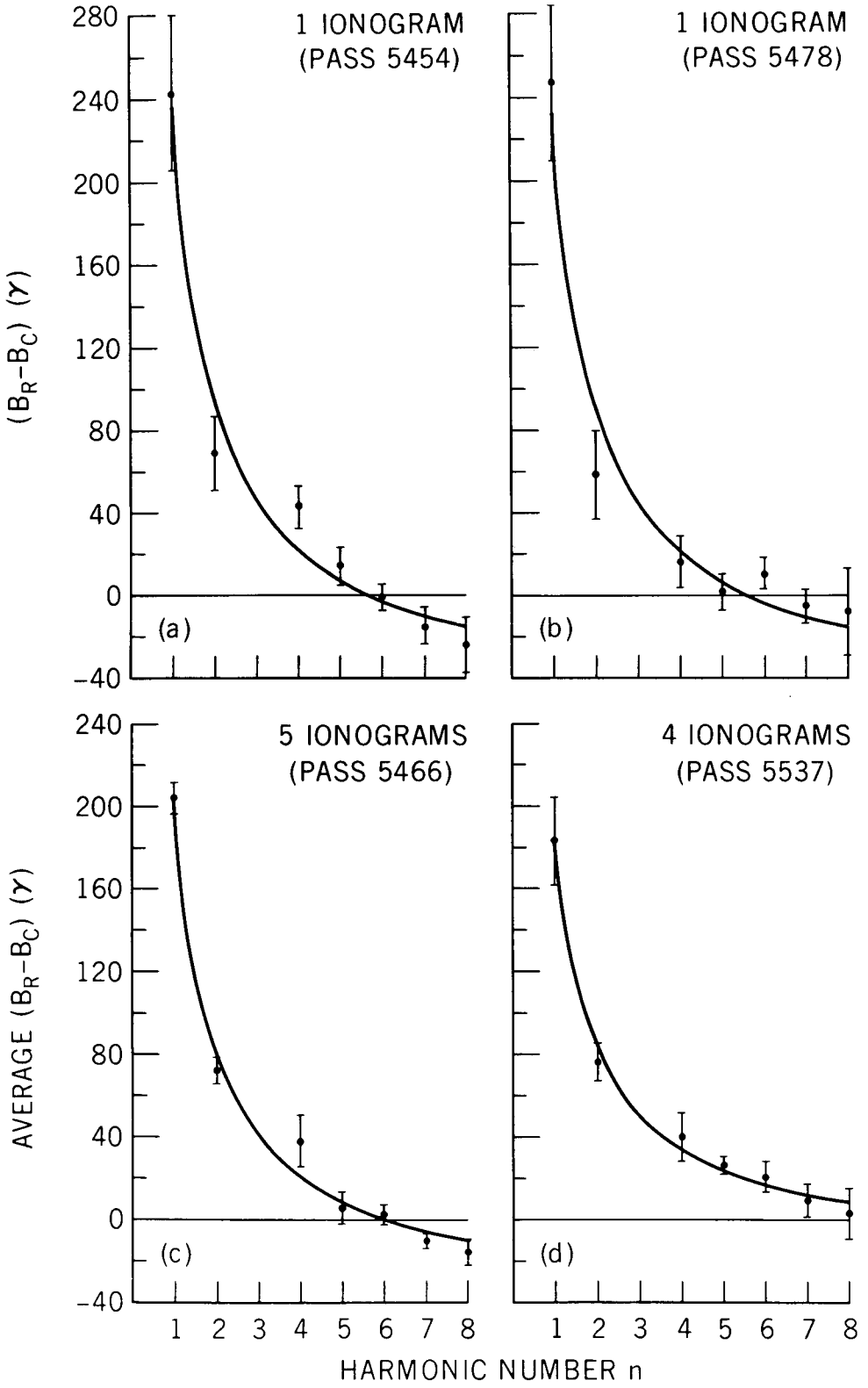

Figure 9. The difference field vs. harmonic number n for 2 individual ionograms from separate passes in (a) and (b) and for averaged data from consecutive ionograms from separate passes in (c) and (d). The data correspond to apogee passes near the dipole equator [Benson, 1969]. (Note: the difference between the values in this figure and the values in Figure 4 of Benson [1969] is due to the use of different values for the frequency marker correction term; a correction term of −3.75 kHz, based on Franklin [1970], was used in the original work and −3.0 kHz, based on Franklin and Maclean [1969] and Franklin [personal communication, 1970], in the present work.) See the text for a description of the curves.